THE JOURNAL OF BIOLOGICAL CHEMISTRY VOL. 281, NO. 14, pp. 9400–9406, April 7, 2006

Formation, Structure, and Dissociation of the Ribonuclease S Three-dimensional Domain-swapped Dimer*[S]

Received for publication, September 26, 2005, and in revised form, January 10, 2006 Published, JBC Papers in Press, January 16, 2006, DOI 10.1074/jbc.M510491200

Jorge P. López-Alonso[‡1], Marta Bruix[‡], Josep Font[§2], Marc Ribó[§], María Vilanova[§], Manuel Rico[‡], Giovanni Gotte[¶], Massimo Libonati[¶], Carlos González[‡], and Douglas V. Laurents[‡3]

From the [‡]Instituto de Química-Física "Rocasolano" CSIC, Serrano 119, E-28006 Madrid, Spain, [§]Laboratori d'Enginyeria de Proteïnes, Departament de Biologia, Facultat de Ciències, Universitat de Girona, Campus de Montilivi, E-17071 Girona, Catalunya, Spain, and [¶]Dipartimento di Scienze Neurologiche e della Visione, Sezione di Chimica Biologica, Facoltà di Medicina e Chirurgia dell'Università di Verona, Strada Le Grazie 8, I-37134 Verona, Italy

Post-translational events, such as proteolysis, are believed to play essential roles in amyloid formation *in vivo*. Ribonuclease A forms oligomers by the three-dimensional domain-swapping mechanism. Here, we demonstrate the ability of ribonuclease S, a proteolytically cleaved form of ribonuclease A, to oligomerize efficiently. This unexpected capacity has been investigated to study the effect of proteolysis on oligomerization and amyloid formation. The yield of the RNase S dimer was found to be significantly higher than that of RNase A dimers, which suggests that proteolysis can activate oligomerization via the three-dimensional domain-swapping mechanism. Characterization by chromatography, enzymatic assays, and NMR spectroscopy indicate that the structure of the RNase S dimer is similar to that of the RNase A C-dimer. The RNase S dimer dissociates much more readily than the RNase A C-dimer does. By measuring the dissociation rate as a function of temperature, the activation enthalpy and entropy for RNase S dimer dissociation were found to resemble those for the release of the small fragment (S-peptide) from monomeric RNase S. Excess S-peptide strongly slows RNase S dimer dissociation. These results strongly suggest that S-peptide release is the rate-limiting step of RNase S dimer dissociation.

Three-dimensional domain swapping is a common mechanism for oligomerization with important implications for protein evolution and amyloid formation (1). In this mechanism, two monomers trade structural motifs, called "swap domains," which adopt essentially identical conformations in the monomeric and oligomeric forms; for recent reviews see Refs. 2 and 3. The swap "domains" can range in size from a single α-helix or β-strand to large protein domains. Domain-swapped oligomers can be stable or metastable relative to their monomers. In the latter case, destabilizing conditions and high protein concentrations typically favor oligomerization by this mechanism. Bovine pancreatic ribonuclease A (RNase A) was the first protein whose oligomerization was proposed to occur by three-dimensional domain swapping (4).

In recent years, investigation of RNase A oligomerization has shown that this protein can form a variety of dimers, trimers, and higher oligomers (5) via three-dimensional domain swapping of the N-terminal α-helix (called N-dimer), the C-terminal β-strand (named C-dimer), or both (6–9) (see supplemental Fig. 1 for ribbon drawings of their crystal structures). The oligomerization of RNase A has been reviewed recently (10). The observation of a new two-stranded β-sheet with an amyloid-like conformation present in the C-dimer of RNase A led Eisenberg and co-workers (7) to propose a model for amyloid formation based on three-dimensional domain swapping. This hypothesis has been supported by the structural characterization of domain-swapped oligomers of amyloid-forming proteins (11, 12) and is now essentially confirmed by very recent work from Eisenberg's laboratory showing that an RNase A variant with a polyglutamine insertion into the C-terminal hinge loop forms amyloid fibrils by three-dimensional domain swapping (13).

RNase A oligomerization can be induced by lyophilization from 40% acetic acid (4) or incubation in heated alcohol/water solutions (14). Moreover, Park and Raines (15) have shown that RNase A can dimerize in heated water without cosolvents, which suggests the existence of small amounts of dimeric RNase A *in vivo*. All RNase A oligomers formed are metastable and slowly dissociate into monomers. The swap domains, which consist of residues 1–15 in the N-dimer and 116–124 in the C-dimer, have the same secondary and tertiary structures regardless of whether they are bound to their own protein core in the monomer or to the alternate core in the oligomer. In contrast, their respective hinge loops, formed by residues 16–22 in the N-dimer and 112–115 in the C-dimer adopt strikingly different conformations in the dimers *versus* the monomer.

RNase A is cleaved at the peptide bond between residues 20 and 21 by subtilisin (16). The small fragment (residues 1–20, named S-peptide) and the large one (residues 21–124, S-protein) remain tightly associated by non-covalent interactions. This complex, RNase S, conserves the catalytic activity (16) and native conformation (17–19) of uncleaved RNase A but shows a reduced conformational stability (20–22).

Although N-terminal domain swapping cannot occur, RNase S monomers might still be able to oligomerize by swapping C termini, which are not cut by subtilisin. However, given the reduced conformational stability of RNase S, many would not expect it to form oligomers. Here, we describe the discovery of RNase S dimers; this is the first reported case, to our knowledge, of a two-chain protein that oligomerizes via the three-dimensional domain-swapping mechanism. The main objectives of this present work are to (i) compare the ability of RNase S to form domain-swapped oligomers relative to RNase A, (ii) characterize the structure of the RNase S dimer, and (iii) measure the kinetics and thermodynamics of RNase S dimer dissociation and propose a mechanism for this process.

* This work supported in part by the MCyT (Spain) (CTQ2004-08275-C02-02, BMC2003-08145-CO2-02 (to M. V.)), the DGR, Generalitat de Catalunya (SGR-01-00196) (to M. V.), by the Italian M.U.R.S.T.-PRIN 2004 (to M. L.), and by support from Prof. J. Santoro (MCyT BIO2002-00720). The costs of publication of this article were defrayed in part by the payment of page charges. This article must therefore be hereby marked "*advertisement*" in accordance with 18 U.S.C. Section 1734 solely to indicate this fact.

[S] The on-line version of this article (available at http://www.jbc.org) contains supplemental figures and tables.

[1] Received a fellowship from the Consejería de Educación de la Comunidad de Madrid y el Fondo Social Europeo.

[2] Received a fellowship from the Universitat de Girona.

[3] A Ramón y Cajal fellow (Spain). To whom correspondence should be addressed. Tel.: 34-91-561-9400; Fax: 34-91-564-2431; E-mail: dlaurents@iqfr.csic.es.

EXPERIMENTAL PROCEDURES

Materials—Bovine pancreatic ribonuclease A (grade XII-A, lot 104H-7110) was obtained from Sigma and further purified by cation-exchange chromatography as described (5) prior to use. Bovine pancreatic ribonuclease S (grade XII-S, lot 106F-8055), S-peptide (grade XII-PE, lot 99F8205), and S-protein (grade XII-PR, lot 125C8045) also obtained from Sigma, eluted as single peaks from a cation exchange column and were used as supplied. Recombinant RNase A uniformly labeled with ^{15}N or ^{15}N and ^{13}C was prepared as described previously (23) using labeled Martek9 medium from Spectra Stable Isotopes. Na_2HPO_4 and NaH_2PO_4 were obtained from Merck and combined in equal molar proportions to give a solution that is 0.20 M in total P_i and has a pH of 6.7. Double-distilled water was deionized using a MilliQ system. All other reagents were the highest purity grade available.

Oligomer Formation—The ability of RNase S and S-protein to form oligomers was tested using two procedures that efficiently induce oligomerization of RNase A; namely (i) incubation in 40% glacial acetic acid, 60% water for 1 h, followed by lyophilization (4) (HAc/lyophilization) and (ii) high temperature incubation in 40% ethanol, 60% water at high protein concentrations (50–200 mg/ml) (EtOH/heat) (14). Incubation temperatures ranging from 30 to 60 °C were tested. NaP_i buffer (0.2 M, pH 6.7) was added to the samples after lyophilization or heat treatment. P_i binds to His^{12} and His^{119} at the active site (24); because these residues are contributed by different monomers, P_i binding stabilizes domain-swapped oligomers of RNase as does the binding of DNA (25).

Chromatography—All chromatography experiments were performed on an Amersham Biosciences ΔKTA FPLC system at ambient temperature (18–20 °C) using Mono S 5/5 and Superdex HR 75 10/30 columns for cation exchange and gel filtration, respectively. Cation exchange chromatography was carried out by applying a linear gradient of 20–200 mM NaP_i (pH 6.70) as previously described (14). Gel filtration was performed in 0.2 M NaP_i buffer. Elution volume determination and peak integration was performed using the Amersham Biosciences Unicorn software.

Thermal Denaturation—Thermal transitions (0–70 °C) of RNase S and RNase A (≈0.5 mg/ml) in 40% ethanol, 60% water were recorded in a 0.1-cm cuvette using a JASCO J-810 circular dichroism spectrometer equipped with a Peltier temperature control unit. These samples were unbuffered, pH ≈ 6.8, to be consistent with the EtOH/heat oligomerization conditions. The scan speed was 60 °C/h. The reversibility of unfolding was checked by recording the ellipticity during recooling to 0 °C and was found to be better than 95%. The data shown are representative of four independent experiments.

Enzyme Kinetics—The enzymatic activities of ribonuclease monomers and dimers were measured against single stranded yeast RNA (ssRNA)[4] using the Kunitz assay (26) and against synthetic double stranded RNA, poly(A)·poly(U) as previously described (27). All assays were repeated in duplicate, and the uncertainty of these activity values is typically ~±7% and ±15%, against ssRNA and poly(A)·poly(U), respectively (5). Because gel filtration analysis found that the RNase S dimer sample contained 56% dimer and 44% monomer, the activity of 100% dimer was calculated by subtracting the activity due to monomer from the observed activity and then dividing by the fraction of dimer. The specific activity values were then normalized to the RNase A monomer.

Nuclear Magnetic Resonance—All NMR spectra were recorded at 25.0 °C, in NaP_i buffer (0.2 M, pH 6.7) containing 90% H_2O, 10% D_2O or in 99.9% D_2O using the most upfield resonance of sodium 4,4-dimethyl-4-silapentane-1-sulfonate as the internal chemical shift reference on a Bruker 800 MHz Avance US[2] NMR spectrometer equipped with a triple resonance (^1H,^{13}C,^{15}N) probe and X, Y, Z-gradients. Three-dimensional ^{13}C,^{15}N,^1H NHCOCA, NHCA, and NHCACB spectra were recorded on a monomeric RNase A sample uniformly labeled in ^{13}C and ^{15}N. Peak assignments were made by following standard procedures in combination with comparison of previous assignments (18, 21). Based on these assignments, two-dimensional ^1H NOESY (mixing time = 50 ms), COSY, and total correlation spectroscopy spectra of monomeric and dimeric RNase S were recorded and assigned in the same solution conditions and temperature. The assignments are deposited in the BMRB data bank. RNase S dimer samples for NMR contained an excess of S-peptide to slow dissociation (see below).

Structural Modeling of the RNase S Dimer—The chemical shift and NOE data sets of RNase A, RNase S, and the RNase S dimer are almost identical; significant differences are only observed near the subtilisin cleavage site (see Fig. 2 in Neira *et al.* (21)) and in the C-terminal hinge loop (see Fig. 2, above). Therefore, their tertiary structures are very similar except at those sites. Starting from two RNase A solution structures, the RNase S dimer structure was modeled by cleaving the 20–21 peptide bonds and then changing the backbone torsion angles of the C-terminal hinge loop to a C-dimer-like conformation using the program Sybyl (Tripos, Inc.). This model was refined with extensive (500 ps) MD simulations with explicit solvent. For further details, see Ref. 28 and the supplemental information.

Dimer Dissociation—The kinetics of the separation of RNase S dimers, in NaP_i buffer (0.2 M, pH 6.7), into monomers was monitored by gel filtration analysis of aliquots incubated at 0, 19.0, 25.0, 31.2, and 37.0 °C. To determine the dissociation rate constant, k, a least-squares algorithm was used to fit first order kinetic rate equations to the experimentally observed increase in monomer (M) or the decrease in dimer (D) with time (t),

$$D(t) = D(t = 0)\exp^{-kt} + D(t = \infty) \qquad \text{(Eq. 1)}$$

and,

$$M(t) = (1 - M(t = 0))\exp^{-kt} + M(t = \infty) \qquad \text{(Eq. 2)}$$

The rate constants (k) as a function of the inverse of the absolute temperature (T) were analyzed using the linear form of the Arrehenius equation,

$$\ln k = -\Delta H^{\ddagger}/RT + \Delta S^{\ddagger}/R \qquad \text{(Eq. 3)}$$

to determine the apparent activation enthalpy ($\Delta H^{\ddagger}$) and entropy ($\Delta S^{\ddagger}$) for rate-limiting step of RNase S dimer dissociation.

RESULTS

RNase S Oligomerizes under Conditions That Induce RNase A Oligomerization

HAc/Lyophilization-induced Oligomerization—To test whether or not RNase S can form three-dimensional domain-swapped oligomers under the conditions that induce oligomerization of RNase A, samples of both proteins were subjected to HAc/lyophilization treatment, and the subsequent products were separated by chromatography (Fig. 1). Cation exchange chromatography was tried first, because it highly resolves RNase A oligomers (5). Here, a very good separation of RNase A oligomers was also obtained with a 0.02–0.20 M NaP_i gradient, and

[4] The abbreviations used are: ssRNA, single stranded RNA; NOE, nuclear Overhauser effect; NOESY, NOE spectroscopy; MD, molecular dynamics; MOPS, 4-morpholinepropanesulfonic acid.

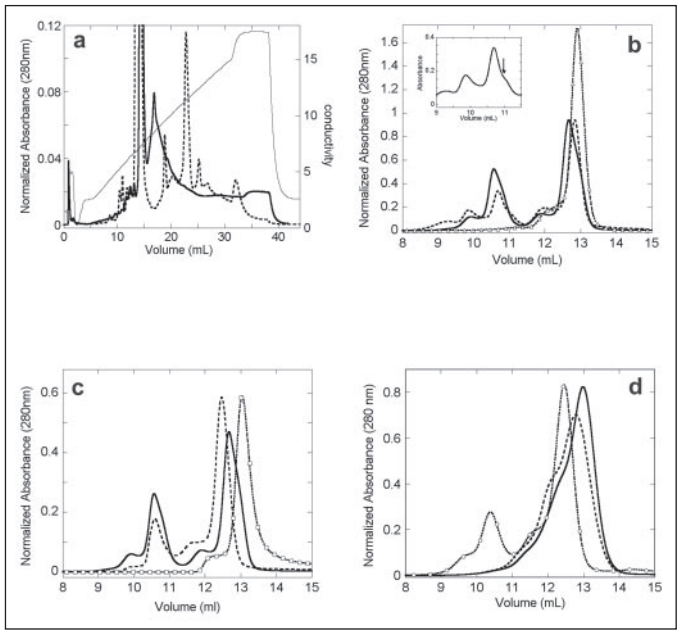

FIGURE 1. **Chromatographic characterization of RNase oligomers.** *a*, cation exchange chromatograms of RNase A (left *y* axis, *dashed line*) and RNase S (left *y* axis, *thick solid line*) after oligomerization by HAc/lyophilization. The conductivity (*thin solid line*, right *y* axis) is proportional to the concentration of NaP_i used in the gradient (20–200 mM). The large off scale peaks eluting ≈13–14 ml are the monomeric forms of RNase A and S and have normalized absorbance values ≈0.45. To facilitate the comparison of the chromatograms in *b–d*, their absorbance was normalized by dividing by the total integral of the raw absorbance. *b*, separation of RNase A (*dashed line*) and RNase S (*solid line*) previously oligomerized by HAc/lyophilization treatment by gel filtration chromatography. For comparison, a sample of untreated RNase S (*dotted line* and *open triangles*) is also shown. *Inset*, the chromatogram of RNase A, expanding the region where tetramers, trimers, and dimers elute. An inflection point (*arrow*) indicates the partial resolution of the C-dimer (*main peak*) from the N-dimer (*shoulder* on the right-hand side) by gel filtration. This inflection point and the N-dimer shoulder are not seen in chromatograms of oligomerized RNase S. The peak eluting near 12.0 ml appears to be because of one or more intermediate species that form during the conversion of dimer into monomer, which seem to behave like monomer after isolation. *c*, RNase S oligomer recovery depends on the concentration of NaP_i. Gel filtration chromatograms of RNase S after oligomerization via HAc/lyophilization in a column equilibrated in 200 mM NaP_i (*solid line*), 90 mM NaP_i (*dashed line*) and 10 mM NaP_i (*dotted line* and *squares*). The variation in the elution volume with NaP_i and the trailing shoulder of the chromatogram in 10 mM NaP_i could be because of variations in the interactions between the protein and the column matrix because of differences in the ionic strength. In *b–d*, no significant absorbance was detected between 0 and 8 ml; the column exclusion volume is ≈7.5 ml. *d*, oligomer formation by S-protein. *Solid line*, untreated S-protein; *dashed line*, HAc/lyophilization treated S-protein, dissolved in NaP_i buffer; *dotted line* with *open circles*, HAc/lyophilization treated S-protein dissolved in NaP_i buffer containing S-peptide.

the elution positions and oligomer yields are consistent with previous results (5, 10) (Fig. 1*a*). However, in the case of HAc/lyophilization treated RNase S, a single peak with a long trailing shoulder was observed to elute soon after the main monomeric peak. Next, the separation of the oligomerization products was attempted using a gel filtration column equilibrated in 200 mM NaP_i. As previously observed (5), RNase A tetramers elute earliest, followed by trimers, the C-dimer, the N-dimer, and finally the monomer (Fig. 1*b*). The ability to partly resolve the two dimers of RNase A by gel filtration is likely because of the more elongated shape of the C-dimer (Fig. 1*b*, *inset*). The chromatogram of RNase S, oligomerized by the HAc/lyophilization procedure, reveals the presence of two peaks, which elute before monomeric RNase S and that were not observed in untreated RNase S (Fig. 1*b*). The smaller peak, whose yield is ~5 ± 1% (1σ, n = 11), has an elution volume that corresponds approximately to a trimeric species. The major RNase S oligomer is probably a dimer, as it elutes 2.08 ± 0.02 ml (1σ, n = 32) before monomeric RNase S, whereas the RNase A N-dimer and C-dimer elute 1.90 ± 0.02 ml and 2.15 ± 0.01 mσ (1 s, n = 4), respectively, before the RNase A monomer. This putative dimer is referred to henceforth as the RNase S dimer. It is remarkable that the yield of the RNase S dimer (32 ± 3%, 1σ, n = 11) is significantly higher than that of the RNase A C-dimer (18 ± 1%) (29) and is even marginally superior to the typical yields (26–30%) (10) of the sum of all the RNase A oligomers formed after HAc/lyophilization treatment.

The stability of the interactions maintaining the quaternary structure of the RNase S oligomers could be low. Phosphate binding to the active site of RNase oligomers cross-links the subunits and thereby stabilizes them. RNase S oligomers might have been present but dissociated in the early stages of cation exchange chromatography, where the concentration of P_i is minimal. To test this possibility, the products of RNase S oligomerization were applied to gel filtration column equilibrated with 200, 90, or 10 mM NaP_i buffer (Fig. 1*c*). The recovery of oligomers decreases substantially as the P_i concentration is lowered.

S-protein might be able to oligomerize because it contains the C-terminal swap domain of RNase A. HAc/lyophilization-treated S-protein analyzed by gel filtration yielded a broad peak whose elution volume is close to that of the RNase S monomer (Fig. 1*d*). The shoulder preceding the elution of the main peak is more prominent for the HAc/lyophilization-treated S-protein than for untreated S-protein; this shoulder might possibly be because of S-protein oligomers, which dissociate into monomers during the chromatography run. A strikingly different result is obtained, however, if a 1.3 molar excess of S-peptide is included in the NaP_i buffer used to redissolve the lyophilized S-protein powder; namely, significant amounts of oligomers are detected (Fig. 1*d*). These results strongly suggest that S-protein can oligomerize by three-dimensional domain swapping of the C-terminal β-strand, as does RNase A, but that S-protein oligomers are much less stable.

Formation of RNase S Oligomers in Heated 40% EtOH—Oligomer formation by RNase S was also found to occur when the protein was incubated at elevated temperatures in 40% ethanol. The average percent oligomer yields as a function of the incubation temperature are shown in Fig. 2*a*. The highest yields of oligomers are obtained near 40 °C for RNase S but at a much higher temperature, ~60 °C, for RNase A (14).

To gain further insight, the thermal denaturation in 40% ethanol of RNase A and S, the concentration of the latter being 43 μM, was followed by CD and thermal midpoint (T_M) values of 30.7 ± 0.2 °C for RNase S and 42.0 ± 0.2 °C for RNase A were obtained (Fig. 2*b*). The T_M value for RNase S is concentration-dependent; when corrected for its concentration under oligomerization conditions (7.3 mM) using the expression of Catanzano *et al.* (20) increases to ≈41 °C (see the supplemental text for additional data analysis details). Altogether, these data suggest that RNase A oligomerizes most efficiently at high temperatures where it is completely denatured, whereas RNase S oligomerization is highest at physiological temperatures near the midpoint of its unfolding transition.

Structural Characterization of the RNase S Dimer

Enzymatic Activities—Because the catalytic activities of RNase A depend strictly on its tertiary and quaternary structure (10), enzymatic assays can shed light on the nature of the RNase S dimer structure. First, both the monomeric and dimeric species of RNase A and RNase S were assayed against yeast ssRNA. The RNase S dimer shows significant activity against ssRNA, which parallels that shown by the RNase A C-dimer (data not shown) and constitutes good evidence that the subunits of the dimer have correctly folded tertiary structures.

The RNase A C-dimer shows a remarkably increased activity against poly(A)·poly(U) relative to the monomer, whereas the enhanced activity of the N-dimer against poly(A)·poly(U) is much smaller (9, 30). Against poly(A)·poly(U), the RNase S dimer demonstrated a strongly enhanced

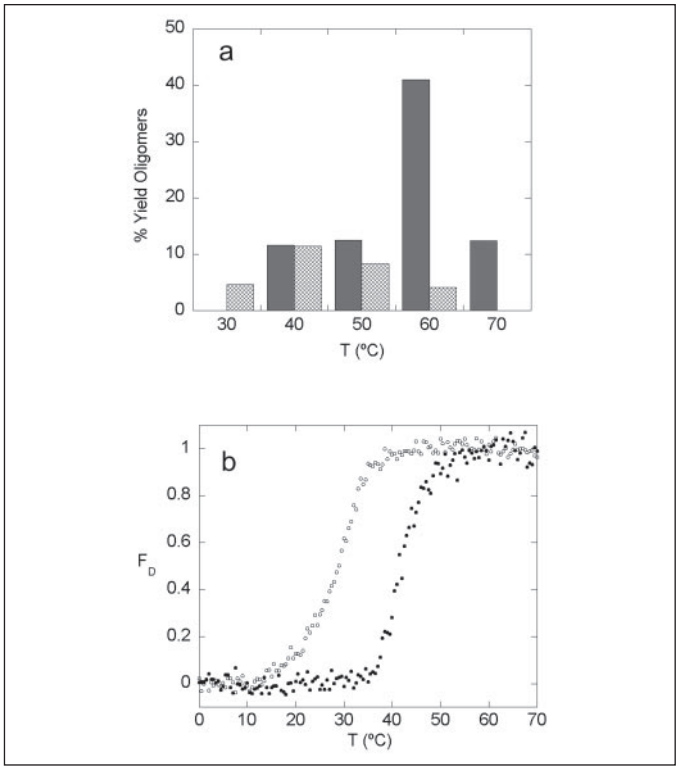

FIGURE 2. **Formation of oligomers via EtOH treatment and thermal stability in 40% ethanol of RNase A and RNase S.** *a*, yield of oligomers obtained from EtOH/heat treatment. RNase A, *filled bars* (data adapted from Ref. 14); RNase S, *dashed line bars*. *b*, thermal denaturation in 40% ethanol. RNase A, *filled circles*; RNase S, *open circles*. The *y* axis label F_D stands for "fraction denatured". The protein concentration was ~0.5 mg/ml.

activity like that of the RNase A C-dimer when assayed side-by-side (Fig. 3*a*).

Structural Characterization by NMR—The aromatic region of the two-dimensional NOESY ^{1}H spectra of the RNase S monomer and dimer are shown in Fig. 3*b*. Although the chemical shifts of most peaks are essentially identical, those of the RNase S dimer are broader, which reflects its slower tumbling in solution. The ring protons of Tyr^{115}, a residue located in the C-terminal hinge loop, alter their chemical shifts in the RNase S dimer relative to the monomer (Fig. 3*b*). The Tyr^{115} ^{1}Hδs and Cys^{58} ^{1}Hβs have strong NOE signals in the monomeric forms of RNase S and A, which are absent in the spectra of the RNase S dimer (Fig. 3*b*) as well as the C-dimer of RNase A (data not shown).

The differences in the backbone chemical shifts of monomeric *versus* dimeric RNase S are small, except in the hinge loop region where significant differences are observed (Fig. 3*c*). As NMR chemical shifts are exquisitely sensitive to conformation, these data indicate that the backbone structure of the monomer and dimer are similar, except in the hinge loop region. A key conformational difference in the hinge loop is revealed by the NOESY spectroscopy. Strong Asn^{113} ^{1}Hα-Pro^{114} ^{1}H,H′ δ NOE signals, which are diagnostic of a *trans* peptide bond, are observed in the RNase S dimer spectrum but are absent in the monomer spectrum (Fig. 3*d*). Similar NOEs are observed for the RNase A C-dimer but are absent in RNase A monomer and N-dimer NOESY spectra (data not shown).

The NMR signals that are characteristic for C-terminal domain swapping, namely those of the Tyr^{115} side chain and NOE signals between the Asn^{113} ^{1}Hα-Pro^{114} ^{1}H,H′ δ, are lost when the RNase S dimer dissociates (see the supplemental text describing additional NMR experiments).

Hydrogen Exchange—Some 30 amide protons in the RNase S dimer resist exchange for more than 2.5 h at pH 6.7, 25 °C when the protein is

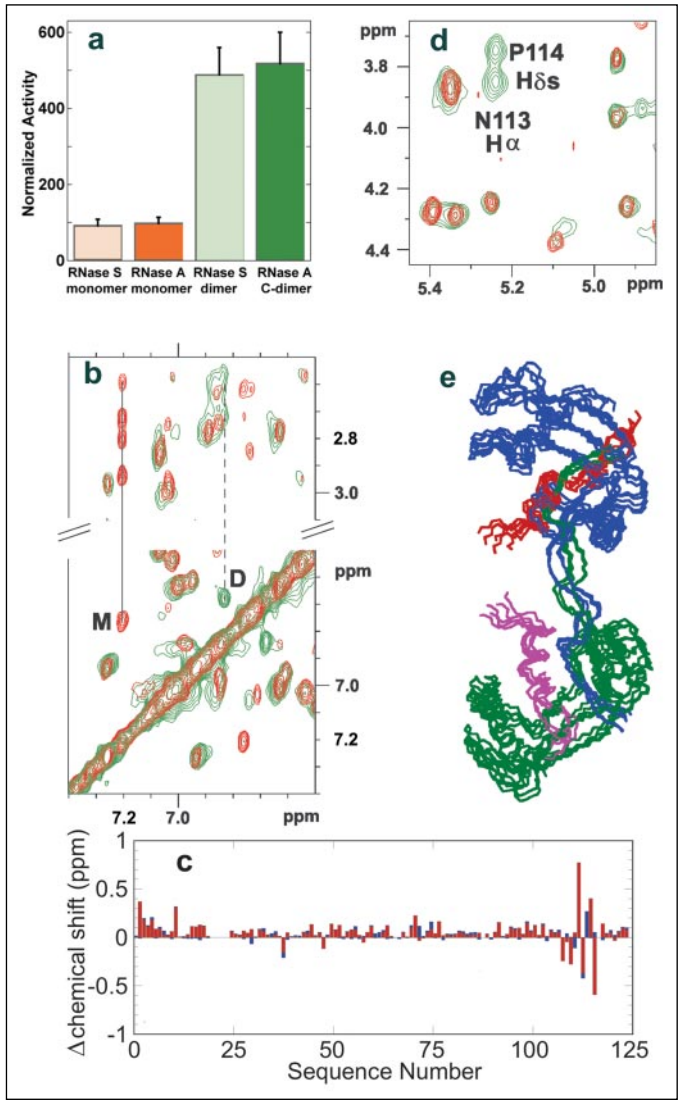

FIGURE 3. **Structural characterization of the RNase S dimer.** *a*, enzymatic activity against poly(A)·poly(U) normalized to monomeric RNase A, whose specific activity was found to be 3.4. *b*, regions of NOESY spectra of the RNase S monomer (*red*) and dimer (*green*). The Tyr^{115} ^{1}Hδ-^{1}Hϵ cross-peak is labeled with an M (monomer) and a D (dimer). A *solid line* (monomer) shows the cross-peaks to the Cys^{58} ^{1}Hβs (2.82 and 2.94 ppm), which are absent for the dimer (*dashed line*). *c*, backbone chemical shift differences between the dimeric and monomeric forms of RNase S: N^{1}H (*red*), ^{1}Hα (*blue*). *d*, region of NOESY spectra of the RNase S monomer (*red*) and dimer (*green*). Cross-peaks due to Asn^{113} ^{1}Hα (5.23 ppm, *x* axis) to Pro^{114} ^{1}Hδs (3.74, 3.83 ppm, *y* axis) in dimeric RNase S are labeled. *e*, structural model of the RNase S dimer. S-protein subunits are shown in *green* and *blue*, and the S-peptides are shown in *magenta* and *red*. Five structures, snapshots of the MD calculation at 100-ps intervals, are shown.

dissolved in D_2O but are fully exchanged after 14 h. Based on these observations, protection factors on the order of 10^5-10^6 can be estimated for these protons. These values are comparable to those previously reported for the RNase S monomer (21, 22), and this resemblance suggests that the conformational stabilities of the RNase S monomer and dimer are also similar. The identities of the highly protected protons match closely in the RNase S monomer and dimer; this is an additional indication that they share similar tertiary structures (see supplemental Table 1 for a list of the protected amide protons in the monomer and dimer).

Structural Model—A structure of the RNase S dimer modeled on the basis of the NMR data is shown in Fig. 3*e*. Overall, the structure is very similar to the C-dimer of RNase A (7), cleaved between Ala^{20} and Ser^{21} in the two subunits. The evolution of the structure during the course of

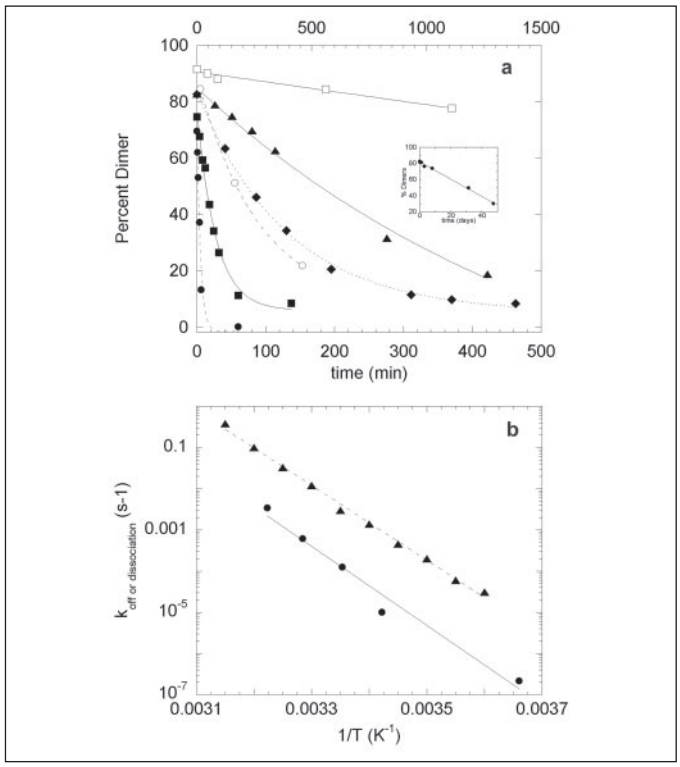

FIGURE 4. **The kinetics and thermodynamics of RNase S dissociation.** *a*, dissociation kinetics of RNase S dimer at 37.0 °C, *solid circle*, *dashed line*; 31.2 °C, *solid square*, *solid line*; 25.0 °C, *solid diamond*, *dotted line*; 19.0 °C, *solid triangle*, *solid line*. RNase S + 3-fold excess of S-peptide: 37.0 °C *open circle*, *dashed line*; 31.2 °C *open square*, *solid line*. Bottom *x* axis 37.0, 31.2, and 25.0 °C; Top *x* axis 19.0 °C. The *inset* shows dissociation of RNase S dimers at 0 °C. The symbols correspond to the experimental data, and the curve shown is the fit of the rate equation. The reproducibility of the percentage of dimer measured is ≤1% and is smaller than the symbols shown. *b*, linear Arrhenius plot of the dissociation rate of the RNase S dimer (*solid circles*, *solid line*) and the dissociation of S-peptide from monomeric RNase S (*solid triangles*, *dashed line*; adapted from (31)). The experimental uncertainties in the rate and temperature are smaller than the symbols shown.

the MD simulation (shown in supplemental Fig. 2) suggests that it is well folded and contains no strained regions.

RNase S Dimer Dissociation

Dissociation Kinetics—The stability of the RNase S dimers against dissociation upon incubation at various temperatures was monitored by gel filtration chromatography, and the results are shown in Fig. 4*a*. Essentially equivalent rate constants were found by fitting the increase in monomer or the decrease in dimer with time (data not shown). The dissociation kinetics depend strongly on temperature, with the kinetic lifetimes at 0 and 37 °C being: $\tau_{0°} = 78{,}000 \pm 1500$ min (54 ± 1 days) and $\tau_{37°} = 5 \pm 1.5$ min, respectively. In comparison, the monomerization of the RNase A C-dimer is very slow under these conditions. After 1 month at 37 °C in 0.20 M NaP_i, pH 6.7, less than 10% had dissociated into monomers (data not shown). The ability of additional S-peptide to stabilize the RNase S dimers was also tested. When a 3-fold molar excess of S-peptide was added to RNase S dimers, their dissociation kinetics slowed dramatically. At 31.2 °C with a 3-fold excess of S-peptide, less than 25% of the RNase S dimer dissociates after 3 h, whereas without additional S-peptide, the dimer has essentially completely disassociated after 2 h (Fig. 4*a*). At 37 °C, a 3-fold molar excess of S-peptide reduces the RNase S dissociation rate 20-fold, with $\tau_{37°,\ 3\times\ S\text{-}pep} = 106 \pm 18$ min.

Thermodynamics of RNase S Dimer Dissociation—Arrhenius plots of the rate of RNase S dimer dissociation and the release of S-peptide from monomeric RNase S determined by Goldberg and Baldwin (31) are shown in Fig. 4*b*. Whereas the slope and intercept of these two data sets are similar, the dissociation of the RNase S dimers is 30–40 times slower than the release of S-peptide from S-protein over the temperature range studied. This difference could be because of the stabilizing action of the 200 mM NaP_i in the buffer used here and replaced by 10 mM MOPS in the work of Goldberg and Baldwin (31). The apparent activation enthalpy and entropy for the dissociation of the RNase S dimers are 43.9 kcal/mol and 130 cal/mol K, respectively, and remarkably similar values of 41.5 kcal/mol ($\Delta H^{\ddagger}$) and 129 cal/mol K ($\Delta S^{\ddagger}$) were reported for the release of S-peptide from RNase S (31).

DISCUSSION

RNase S Forms a Domain-swapped Dimer—A dimeric and a trimeric species of RNase S are observed after HAc/lyophilization or EtOH/heat treatment. These oligomers could be similar to the C-dimer and cyclic trimer of RNase A, which are formed by swapping of the C-terminal β-strand. The ability of S-protein to oligomerize lends further support to the idea that the presence or covalent attachment of the S-peptide moiety is not necessary for C-terminal swapping.

Protease-activated Oligomerization via Three-dimensional Domain Swapping—Proteolytic cleavage enhances the ability of RNase A to oligomerize via three-dimensional domain swapping. Substantially higher dimer yields are obtained for RNase S compared with RNase A from HAc/lyophilization treatment. Moreover, the EtOH/heat treatment appears to produce the highest yields of RNase S oligomers near physiological body temperature, although the recovery of RNase S oligomers could be reduced at high temperature because of an increased tendency to dissociate. In contrast, the optimal oligomerization of RNase A requires much more vigorous heating.

Proteolysis activates oligomerization by destabilizing the native state. In solution, RNase S displays an apparently higher conformational flexibility compared with RNase A, which is in fact because of the presence of minute quantities of dissociated and partly unfolded S-protein and S-peptide (22, 32). As acid or heat promote the dissociation of S-protein and S-peptide, and the loss of S-peptide decreases the stability and conformational integrity of S-protein (33), it is likely that higher populations of partly unfolded S-protein species relative to RNase A species will be present in 40% acetic acid or physiological temperatures and thus account for the higher yields of RNase S dimer. The destabilization of the native state induced by proteolysis is generally because of the greater entropic cost of binding and folding two independent polypeptide chains (34). Partial protein unfolding *in vitro* frequently stimulates the partial or complete conversion into amyloid as described by the "zipper-spine" (7, 35) and "entire-refolding" (36) models. The lack of complete conversion of RNase S into amyloid fibrils is probably because of the rigidity imposed by its four disulfide bonds, as predicted by the zipper-spine model, or the high positive charge of the protein in acetic acid, or both. High net charge impedes the oligomerization of Alzheimer's amyloid peptides (37). The proteolytic cleavage of the amyloid precursor protein produces the Aβ peptide that aggregates into neurotoxic oligomers that play key roles in triggering Alzheimer disease (38). The very recent results of Eisenberg and co-workers (13), which confirm amyloid fibril formation via the domain-swapping mechanism, together with our discovery that domain-swapped oligomerization can be activated by proteolysis, could have far reaching consequences for protein aggregation *in vivo* where essentially all proteins are subject to proteolysis (Fig. 5*a*).

Stabilization by Phosphate—The poor recovery of RNase S dimers by cation exchange chromatography is probably because of the low stability of these dimers at the low $[P_i]$ present early in the separation. A binding constant of 120–150 M^{-1} for P_i to the RNase A active site can be

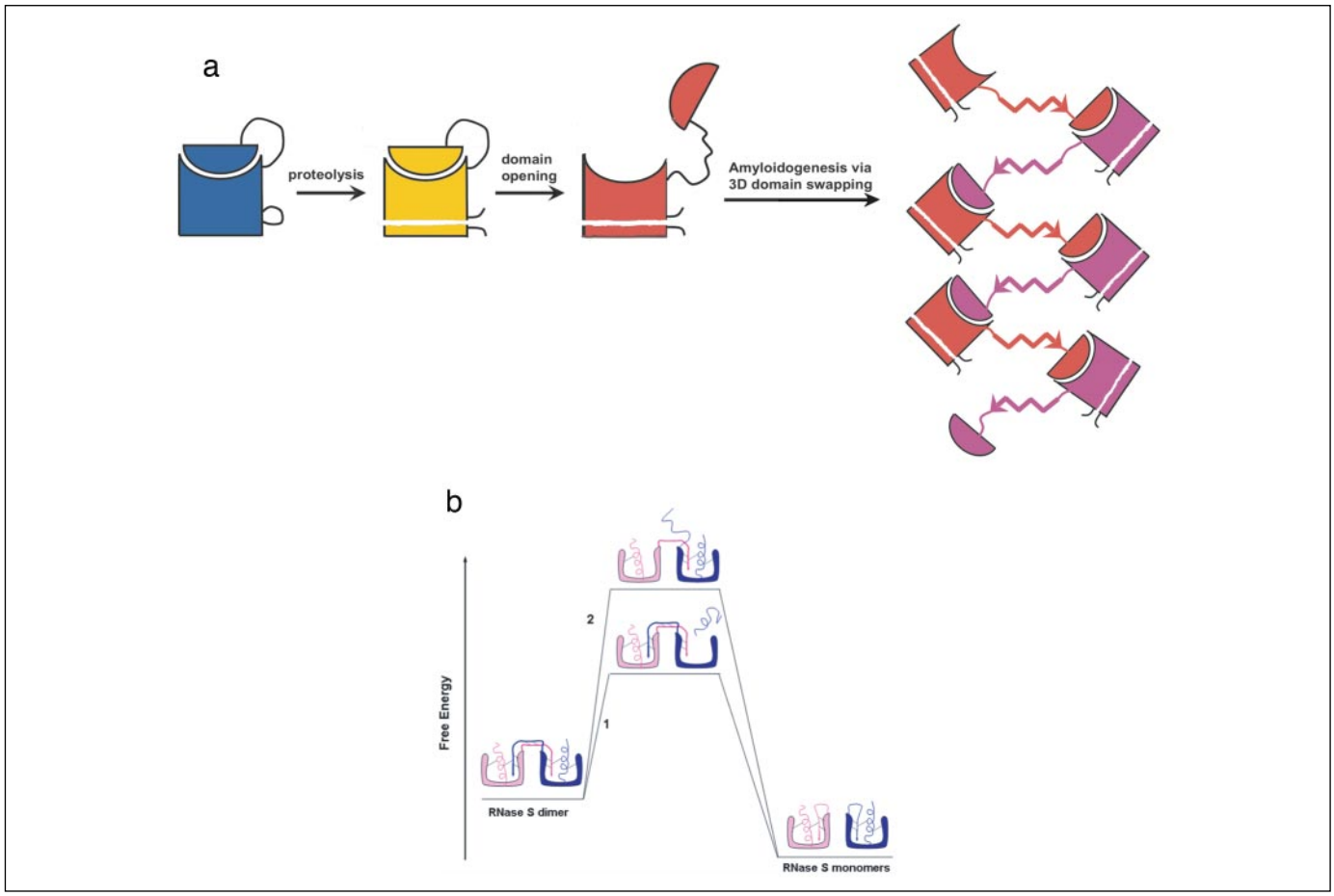

FIGURE 5. **Possible routes for protein aggregation induced by proteolysis and RNase S dimer dissociation.** *a*, plausible, hypothetical mechanism for protease activated three-dimensional domain-swapping-mediated amyloidogenesis. The conformational stability of a protein is decreased when it is cleaved proteolytically, leading to an increase in partially unfolded species that are able to undergo domain swapping. Multiple domain-swapping events could lead to the formation of amyloid fibrils. *b*, plausible mechanisms for RNase S dimer dissociation. Two possible pathways for RNase S dimer dissociation are shown. RNase S dimer dissociation could be rate-limited by the release of a molecule of S-peptide (pathway *1*) or by the separation of a C-terminal β-strand (pathway *2*).

derived from the pK_a shifts of His^{12} and His^{119} upon adding P_i measured by NMR at 22 °C (24). These values are similar to that of 150 M^{-1} determined by calorimetry at 25 °C (20). Using these values and the thermodynamic expression linking selective binding to stabilization (39, 40), the binding of 0.20 M P_i to the RNase S active site is calculated to stabilize the folded conformation by 1.9–2.1 kcal/mol. P_i binding slows RNase S dimer dissociation by linking His^{12} in S-peptide to His^{119} in the swapped C-terminal β-strand. With a binding constant of 150 M^{-1}, at typical concentrations of RNase S present at elution (60 μM) and 0.2 M P_i, it can be estimated that only 3% of the RNase S active sites lack bound P_i, but 25% of the active sites lack P_i at 0.02 M P_i.

The Structure of the RNase S Dimer Is Similar to That of the RNase A C-dimer—The enzymatic activities of the RNase S dimer, both against ssRNA and poly(A)·poly(U) closely match those of the RNase A C-dimer. These results strongly suggest that the tertiary and quaternary structures of the RNase S dimer and the RNase A C-dimer are similar. This conclusion is further supported by the similar elution volumes of these dimers and especially by the evidence provided by NMR spectroscopy, which is the basis for the structural model of the RNase S dimer (Fig. 4*e*). In particular, the backbone conformation of the RNase S dimer and the RNase A C-dimer hinge loops match closely, and the Asn^{113}-Pro^{114} peptide bond is *trans* in both, whereas it is *cis* in the monomers.

Mechanism for Dissociation of the RNase S Dimers—Two possible pathways for RNase S dimer dissociation are depicted in Fig. 5*b*. In pathway *1*, the separation of S-peptide from one subunit is the rate-limiting step for dimer dissociation. This separation will weaken the union between the swapped β-strand and the S-protein moiety, leading to its rapid separation and dissociation of the dimers. In contrast, pathway *2* envisages the separation of a swapped β-strand and hinge loop and the accompanying loss of stabilizing interactions as the rate-limiting step in dissociation.

The ability of free S-peptide (6) and of a peptide corresponding to residues 111–124 of the C terminus (41) to influence the yield of N- and C-dimers, respectively, underscores the importance of local unfolding in both domain-swapping reactions. However, previous studies have shown that the interactions between the protein core and the C-terminal β-strand are stronger than those between the protein core and the N-terminal α-helix or S-peptide moiety. Nine main chain H-bonds link the C-terminal β-strand to the RNase A core compared with two for the S-peptide moiety in the solution (42) and in the crystal (19) structures of RNase A and S. Moreover, the dynamic behaviors of RNase A and RNase S are quite similar, as probed by MD simulation (32), and strong protection against hydrogen exchange is found for amide protons in H-bonds linking the C-terminal swap domain but not the N-terminal swap domain to the protein core (21, 22). Significant protection factors for the former protons are even observed in S-protein (22). The H-bonds formed by the C-terminal β-strand are among the first to form during RNase A folding (43). The reactivation of des-(119–124)-RNase

A by synthetic C-terminal peptides identified residues contributing important hydrophobic interactions (44). The hydrophobic side chains of C-terminal β-strand have been proposed to contribute to the early folding of RNase A (45). Using the protein engineering approach, these side chains have been shown to be key for RNase A stability (46, 47). In contrast, side chain packing occurs late in the binding of S-peptide to S-protein (31). Finally, the observation that the N-dimer of RNase A forms preferentially under moderately destabilizing conditions, whereas the C-dimer formation is favored under strongly destabilizing conditions, was rationalized on the basis that stronger denaturing conditions are needed to detach the C-terminal β-strand (14). All these lines of evidence converge toward the conclusion that the RNase S dimer chiefly dissociates via pathway 1.

Experimental support for dissociation of RNase S dimers following pathway 1 is provided by the finding here that the thermodynamics of RNase S dimer dissociation are similar to those reported for the dissociation of S-peptide from RNase S. Proline isomerization, which might govern the conformational change of the C-terminal hinge loop necessary for dissociation via pathway 2, has a quite different activation enthalpy, ≈20 kcal/mol (48). Finally, the ability of additional S-peptide to slow the dissociation of RNase S dimer and the rapid breakdown of the S-protein dimer in the absence of S-peptide is more consistent with pathway 1 dissociation, because according to transition state theory, the dimer and transition state are in equilibrium; hence it follows from the Le Châtelier Principle that the addition of S-peptide will drive this equilibrium toward the dimer. The relatively slow dissociation rate of the RNase A C-dimer can be understood considering the extremely high local concentration of the segment corresponding to S-peptide.

Acknowledgments—We are grateful to Prof. J. Santoro for implementation of the three-dimensional NMR pulse sequences. The support and encouragement of J. López and M. I. Alonso is appreciated. We gratefully acknowledge the constructive criticism and comments of Prof. G. D'Alessio and Prof. L. Mazzarella made when a preliminary account of this research was presented in the "Seventh International Meeting on Ribonucleases" held in Stará Lesná, Slovak Republic in June 2005.

REFERENCES

1. Bennett, M. J., Schlunegger, M. P., and Eisenberg, D. (1995) *Protein Sci.* **4,** 2455–2468
2. Liu, Y., and Eisenberg, D. (2002) *Protein Sci.* **11,** 1285–1299
3. Rousseau, F., Schymkowitz, J. W., and Itzhaki, L. S. (2003) *Structure* (*Camb.*) **11,** 243–251
4. Crestfield, A. M., Stein, W. H., and Moore, S. (1962) *Arch. Biochem. Biophys.* **1,** (suppl.) 217–222
5. Gotte, G., Bertoldi, M., and Libonati, M. (1999) *Eur. J. Biochem.* **265,** 680–687
6. Liu, Y., Hart, P. J., Schlunegger, M. P., and Eisenberg, D. (1998) *Proc. Natl. Acad. Sci. U. S. A.* **95,** 3437–3442
7. Liu, Y., Gotte, G., Libonati, M., and Eisenberg, D. (2001) *Nat. Struct. Biol.* **8,** 211–214
8. Liu, Y., Gotte, G., Libonati, M., and Eisenberg, D. (2002) *Protein Sci.* **11,** 371–380
9. Gotte, G., and Libonati, M. (2004) *J. Biol. Chem.* **279,** 36670–36679
10. Libonati, M., and Gotte, G. (2004) *Biochem. J.* **380,** 311–327
11. Knaus, K. J., Morillas, M., Swietnicki, W., Malone, M., Surewicz, W. K., and Yee, V. C. (2001) *Nat. Struct. Biol.* **8,** 770–774
12. Janowski, R., Kozak, M., Jankowska, E., Grzonka, Z., Grubb, A., Abrahamson, M., and Jaskolski, M. (2001) *Nat. Struct. Biol.* **8,** 16–20
13. Sambashivan, S., Liu, Y., Sawaya, M. R., Gingery, M., and Eisenberg, D. (2005) *Nature* **437,** 266–269
14. Gotte, G., Vottariello, F., and Libonati, M. (2003) *J. Biol. Chem.* **278,** 10763–10769
15. Park, C., and Raines, R. T. (2000) *Prot. Sci.* **9,** 2026–2033
16. Richards, F. M., and Vithayathil, P. J. (1959) *J. Biol. Chem.* **234,** 1459–1465
17. Wyckoff, H. W., Tsernoglou, D., Hanson, A. W., Knox, J. R., Lee, B., and Richards, F. M. (1970) *J. Biol. Chem.* **245,** 305–328
18. Rico, M., Bruix, M., Santoro, J., González, C., Neira, J. L., Nieto, J. L., and Herranz, J. (1989) *Eur. J. Biochem.* **183,** 623–638
19. Kim, E. E., Varadarajan, R., Wyckoff, H. W., and Richards, F. M. (1992) *Biochemistry* **31,** 12304–12314
20. Catanzano, F., Giancola, C., Graziano, G., and Barone, G. (1996) *Biochemistry* **35,** 13378–13385
21. Neira, J. L., Sevilla, P., Menéndez, M., Bruix, M., and Rico, M. (1999) *J. Mol. Biol.* **285,** 627–643
22. Chakshusmathi, G., Ratnaparkhi, G. S., Mudhu, P. K., and Varadarajan, R. (1999) *Proc. Natl. Acad. Sci. U. S. A.* **96,** 7899–7904
23. Ribó, M., Benito, A., Canals, A., Nogués, M. V., Cuchillo, C. M., and Vilanova, M. (2001) *Methods Enzymol.* **341,** 221–234
24. Cohen, J. S., Griffen, J. H., and Schechter, A. N. (1973) *J. Biol. Chem.* **248,** 4305–4310
25. Nenci, A., Gotte, G., Bertoldi, M., and Libonati, M. (2001) *Protein Sci.* **10,** 2017–2027
26. Kunitz, M. (1946) *J. Biol. Chem.* **164,** 563–568
27. Libonati, M., and Sorrentino, S. (2001) *Methods Enzymol.* **341,** 234–248
28. Gómez-Pinto, I., Cubero, E., Kalko, S. G., Monaco, V., van der Marel, G., van Boom, J. H., Orozco, M., and González, C. (2004) *J. Biol. Chem.* **279,** 24552–24560
29. Gotte, G., Libonati, M., and Laurents, D. V. (2003) *J. Biol. Chem.* **278,** 46241–46251
30. Sorrentino, S., Barone, G., Bucci, E., Gotte, G., Russo, N., Libonati, M., and D'Alessio, G. (2000) *FEBS Lett.* **466,** 35–39
31. Goldberg, J. M., and Baldwin, R. L. (1998) *Biochemistry* **37,** 2556–2563
32. Nadig, G., Ratnaparkhi, G. S., Varadarajan, R., and Vishveshwara, S. (1996) *Protein Sci.* **5,** 2104–2114
33. Graziano, G., Catanzano, F., Giancola, C., and Barone, G. (1996) *Biochemistry* **35,** 13386–13392
34. Tamura, A., and Privolov, P. L. (1997) *J. Mol. Biol.* **273,** 1048–1060
35. Ivanova, M. I., Sawaya, M. R., Gingery, M., Attinger, A., and Eisenberg, D. (2004) *Proc. Natl. Acad. Sci. U. S. A.* **101,** 10584–10589
36. Fändrich, M., Fletcher, M. A., and Dobson, C. M. (2001) *Nature* **410,** 165–166
37. Guo, M., Gorman, P., M, Rico, M., Chakrabartty, A., and Laurents, D. V. (2005) *FEBS Lett.* **579,** 3574–3578
38. Walsh, D., Klyubin, I., Fadeeva, J. V., Cullen, W. K., Anwyl, R., Wolfe, M. S., Rowan, M. J., and Selkoe, D. J. (2002) *Nature* **416,** 535–539
39. Pace, C. N., and McGrath, T. (1980) *J. Biol. Chem.* **255,** 3862–3865
40. Schellman, J. A. (1975) *Biopolymers* **14,** 999–1018
41. Nakano, S.-I., and Sugimoto, N. (2003) *J. Am. Chem. Soc.* **125,** 8728–8729
42. Santoro, J., González, C., Bruix, M., Neira, J. L., Nieto, J. L., Herranz, J. L., and Rico, M. (1993) *J. Mol. Biol.* **229,** 722–734
43. Ungaonkar, J. B., and Baldwin, R. L. (1990) *Proc. Natl. Acad. Sci. U. S. A.* **87,** 8197–8201
44. Lin, M. C., Gutte, B., Caldi, D. G., Moore, S., and Merrifield, R. B. (1972) *J. Biol. Chem.* **247,** 4768–4774
45. Houry, W. A., and Scheraga, H. A. (1996) *Biochemistry* **35,** 11734–11746
46. Torrent, J., Connelly, J. P., Coll, M. G., Ribó, M., Lange, R., and Vilanova, M. (1999) *Biochemistry* **38,** 15952–15961
47. Torrent, J., Rubens, P., Ribo, M., Heremans, K., and Vilanova, M. (2001) *Protein Sci.* **10,** 725–734
48. Schmid, F. X., and Baldwin, R. L. (1978) *Proc. Natl. Acad. Sci. U. S. A.* **75,** 4764–4768
49. Deleted in proof
50. Deleted in proof